Determination of Specific Volume Fractions in Multicomponent Liquids Using Hydrogel-Functionalized Plasmonic Sensors

Julia Herzog, Martin Sobczyk, Christiane Schuster, Thomas Härtling, Thomas Wallmersperger, and Gerald Gerlach

***Abstract*—Plasmonic sensors based on nanostructured metal substrates offer a promising solution for on-site implementation and continuous monitoring of process liquids due to their compact design, cost-effectiveness, and rapid sensor response. The sensors are qualified for the functionalization with biological recognition elements and thus for biosensing. A functionalization with stimulus-responsive hydrogels further enhances their utility by enabling selective determination of specific substances in complex solutions. However, challenges arise in accurately interpreting the sensor signals due to the nonlinearity between the swelling curve of the hydrogel and the sensor signal and due to interferences from nontarget substances. An important objective of this study is to develop a methodology to accurately determine the concentration of a target substance in a multicomponent solution, eliminating the influence of interfering substances. For this, it is imperative to enhance the comprehension of the system, elucidating the impact of the hydrogel's swelling state and the composition on the sensor signal. An analytical model is presented, conveying a linear relationship between the sensor signal and the volume fraction of each constituent in the hydrogel. Based on the proposed model, a novel difference method is established to eliminate the influence of interfering substances, particularly at low concentrations of interfering substances. In a proof-of-concept, using an ethanol-sensitive hydrogel for detection of ethanol in aqueous ethanol–glucose solution, the method was validated, showing a negligible impact of glucose concentration on the result.**

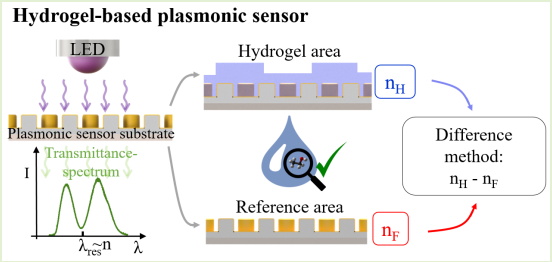

***Index Terms*— Chemical and biological sensors, hydrogels, intelligent materials, nanoplasmonics.**

Manuscript received 19 February 2024; accepted 23 February 2024. Date of publication 5 March 2024; date of current version 1 May 2024. This work was supported in part by German Research Foundation [Deutsche Forschungsgemeinschaft (DFG)] Research Training Group "Hydrogel-based Microsystems" under Grant RTG 1865 and in part by Bundesministerium für Bildung und Forschung (BMBF) Validierung des technologischen und gesellschaftlichen Innovationspotenzials wissenschaftlicher Forschung (VIP)+ Program, under Grant 03VP01970. An earlier version of this paper was presented at the Eurosensors XXXV Conference 2023 and was published in its Proceedings. The associate editor coordinating the review of this article and approving it for publication was Dr. Amir Ebrahimi. *(Corresponding author: Julia Herzog.)*

Julia Herzog and Gerald Gerlach are with the TU Dresden, Institute of Solid-State Electronics, 01069 Dresden, Germany (e-mail: julia.herzog@tu-dresden.de; gerald.gerlach@tu-dresden.de).

Martin Sobczyk and Thomas Wallmersperger are with the TU Dresden, Institute of Solid Mechanics, Chair of Mechanics of Multifunctional Structures, 01069 Dresden, Germany (e-mail: martin.sobczyk@tu-dresden.de; thomas.wallmersperger@tu-dresden.de).

Christiane Schuster is with the Fraunhofer Institute for Ceramic Technologies and Systems IKTS, 01109 Dresden, Germany (e-mail: christiane.schuster@ikts.fraunhofer.de).

Thomas Härtling is with the Fraunhofer Institute for Ceramic Technologies and Systems IKTS, 01109 Dresden, Germany, also with the Institute of Solid-State Electronics, 01069 Dresden, Germany, and also with the Fraunhofer Portugal Center for Smart Agriculture and Water Management AWAM, Parque de Ciência e Tecnologia de Vila Real– Régia Douro Park, 5000-033 Vila Real, Portugal (e-mail: thomas.haertling@ikts.fraunhofer.de).

Digital Object Identifier 10.1109/JSEN.2024.3371095

I. Introduction

APPLICATIONS in fields such as pharmacy, biotechnology, food industry, or environmental engineering require continuous determination of specific substances in complex multicomponent solutions. This is important in order: 1) to comply with limit values in the manufacturing process; 2) to ensure product quality; and 3) to control the process in general. Often, continuous process monitoring is a required feature for process automation. On-site sensors fulfilling criteria such as cost-efficiency, high accuracy, continuous operation, and real-time response are highly desirable for effective monitoring in these applications.

The state of the art for the selective determination of individual substances in multicomponent samples is the use of chromatographs in various setups—gas chromatography, chromatography–mass spectrometry, and (high-performance) liquid chromatography [1], [2], [3], [4]. Such measurement methods allow highly precise determination of substance concentrations, even of multiple substances simultaneously. However, these are costly, time-consuming, centralized analysis methods, unsuitable for continuous determination of fluid constituents.

In the field of scientific research, various sensors for fluid process monitoring are under exploration, each at different stages of applicability. For instance, certain electrochemical sensors demonstrate potential as on-site monitoring tools [5], [6], [7], while others are especially promising for selective determination of individual substances [8], [9]. Microwave sensors are suitable for simultaneous determination of different liquid volume fractions [10], [11], but require complex data evaluation. In addition, optical methods, including near-infrared spectroscopy [12], [13], [14] and colorimetric techniques [15], [16], alongside plasmonic sensors, contribute to this field. Near-infrared spectroscopy allows for rapid and simultaneous determination of substances but necessitates complex and costly spectrometers. Colorimetric methods, on the other hand, offer simplicity but lack the capability for continuous determination of liquid composition. Plasmonic sensors generally offer fast on-site detection with compact setups and high sensitivity while giving the possibility of simultaneous data acquisition and multiplexing. These include surface-enhanced Raman spectroscopy methods [17], [18], optical fiber-based surface plasmon resonance sensors [19], [20], [21], such as WaveFlex biosensors [22], [23], and plasmonic sensors using nanostructured sensor surfaces [24], [25]. Each of the systems mentioned above pose promising approaches for fluid process monitoring.

We aim to contribute to this field by developing a simple and cost-efficient sensor system capable to continuously and selectively determine the fluid constituents in an unknown process fluid, directly at the site of operation and in real-time. To achieve this objective, we propose a nanostructured plasmonic sensor system that is functionalized with stimulus-responsive hydrogels.

Plasmonic sensor systems sensitive to the changes in refractive index operate on the principle of surface plasmon resonance. Surface plasmons are collective electron oscillations induced at the interface between a dielectric and a metal by electromagnetic waves. These can be excited without complex optics using nanostructured plasmonic sensor surfaces, such as gold-coated nanopillars with dimensions smaller than those of the incident light. This enables very compact and simple, as well as low-cost sensor setups, which are suitable for on-site implementations. Moreover, it is possible to apply them in a compact readout platform using double photodiodes for very simple signal evaluation, further reducing the cost and complexity of the sensor setup [26], [27]. To selectively detect the concentration of a single substance using plasmonically active, refractive-index-sensitive sensor systems, a chemical functionalization of the sensor surface is necessary. For this aim, stimulus-responsive hydrogels are suitable, as demonstrated in previous works [25], [28].

Hydrogels are complex 3-D polymer networks capable of absorbing and retaining large amounts of liquid in the interstitial void between their polymer chains. Certain hydrogels respond to the presence of a specific stimulus (e.g., temperature, pH, specific molecules) with a volume phase transition, e.g., an uptake or release of water. The degree of the volume change correlates to the intensity of the respective stimulus. This characteristic finds application in various sensor setups [25], [28], [29], [30]. Stimuli-responsive hydrogels offer some desirable properties for the application in chemical and biological sensors, as they are biocompatible, cost-effective to manufacture, and readily modifiable to enhance the specificity for a targeted stimulus. In the realm of hydrogel-based sensor applications, understanding the swelling kinetics and underlying mechanisms is paramount. Numerical models offer the capability to simulate the complex processes and physical phenomena occurring within the hydrogel. This enables the investigation of the influence of individual parameters or effects on the overall system, without the need for experimental effort or errors associated with conducting experiments. Continuum approaches such as poromechanical models [31], [32], [33], [34], the multifield theory [35], or models based on the theory of porous media [36], [37] contribute significantly to this field, providing a deeper insight into hydrogel-based systems.

To advance the development of the proposed hydrogel-based plasmonic sensor, it is crucial to comprehend how the swelling behavior of the hydrogel, dependent of the target molecule, affects the optical sensor signal. This aspect was investigated in an earlier work [38], wherein an ethanol-sensitive hydrogel was used to analyze aqueous ethanol solutions. It was discovered that the relationship between the ethanol concentration and the optical sensor signal is nonlinear and exhibits an unexpected relationship to the swelling curve of the ethanol-sensitive hydrogel. Due to these challenges and the lack of understanding of the hydrogel-based system, the determination of ethanol concentration was not feasible. This underscores the necessity for a deeper understanding of the intricate interplay between the hydrogel swelling behavior and its impact on the optical sensor signal, particularly in the context of determining a target substance.

Another obstacle encountered in hydrogel-based optical sensor systems arises from the presence of interfering substances within the liquid. Real-world process liquids are typically complex multicomponent fluids containing a manifold of different substances. Upon stimulus-induced swelling of the hydrogel, all the constituents of the liquid will be absorbed into the hydrogel, thereby altering the refractive index of the hydrogel-functionalized surface. As the plasmonic resonance frequency depends, among other parameters, on the near-field refractive index of the surrounding medium (here: the hydrogel) [39], the optical sensor signal is affected by all the constituents of the hydrogel and their respective volume fractions. Consequently, the sensor signal may be impacted by a multitude of interfering substances.

In this study, an important objective is to understand the intricate relationship between the swelling behavior of the hydrogel and the resulting optical sensor signal. In addition, we aim to comprehensively grasp the impact of interfering substances on this signal. With this knowledge, our subsequent endeavor involves the development of a robust methodology geared toward eliminating the influence of interfering substances on the sensor signal. Through this approach, we aim to accurately determine the concentration of the target substance amidst the presence of interfering substances.

To achieve this, we propose an analytical framework to determine the volume fractions of the respective constituents in the hydrogel and the fluid based on the current swelling state of the hydrogel. Using this framework, a linear relationship between the respective volume fractions and the resulting optical sensor signal is obtained.

The proposed analytical description is translated into a difference method, using the refractive index of the fluid and the hydrogel as input signals. The difference in both the signals shows a negligible influence regarding interfering substances, enabling accurate determination of the concentration of the target substance within an unknown fluid.

The proposed method is validated in a proof-of-concept involving simple three-component liquids comprising water, ethanol, and glucose. Here, ethanol acts as the target substance, while glucose represents the entirety of all the interfering and non-cross-sensitive substances in a multicomponent liquid. To functionalize the plasmonic sensor surface, an ethanol-sensitive hydrogel is used. The swelling behavior of the used ethanol-sensitive polyacrylamide hydrogel depends intrinsically on its solubility in the surrounding solvent. As a hydrophilic polymer, polyacrylamide attracts water molecules due to hydrophilic interactions (particularly dipole interactions) with its amide groups. This attraction results in the absorption of water. Conversely, ethanol, with lower polarity than water, does not interact as strongly with the amide groups. This leads to the expulsion of water from the hydrogel, causing a collapse of the polymer network. The presence of glucose neither impacts the solubility of polyacrylamide nor does it interact with the polymer network's functional groups.

By simultaneously measuring the refractive indices n_{H} and n_{F} of the hydrogel and the liquid, the presented difference method demonstrates the ability to reliably and selectively determine the ethanol concentration with virtually negligible influence of glucose.

II. Sensor System

The measurement principle of the used sensor system is based on a plasmonic sensor substrate comprising hexagonally arranged, subwavelength-dimensioned gold nanopillars, which are fabricated by nanoimprinting and sputtering; see Fig. 1. When the electromagnetic field of the incident light of the near-infrared LED matches that of the oscillating electrons on the surface of the nanostructure, wavelength-selective energy absorption occurs. Using a transmission setup, the light transmitted through the nanostructure shows a dip in the detected spectrum. The position of the intensity minimum, the so-called resonance wavelength λ_{res}, also depends on the near-surface refractive index n of the surrounding medium of the nanostructured substrate. When the chemical and physical properties of the surrounding medium change, this also leads to a change in the near-surface refractive index; consequently, the resonance wavelength shifts proportionally to the change in refractive index.

The sensor setup from Fig. 1 features fluidic and optical components. A foil-based sensor substrate including two fluidic channels and four nanostructured, plasmonically active sensor areas are used for simultaneous detection of the refractive-index-sensitive sensor signals. To determine the refractive index n_{H} of the hydrogel, one of the optically sensitive areas in the fluidic channels was functionalized with a microstructured ethanol-sensitive hydrogel. Furthermore, a nonfunctionalized reference area was established in the same fluid channel for detection of the fluid refractive index n_{F}. The reference area can also serve to compensate for temperature fluctuations and other environmental factors equally affecting both the areas.

The described sensor system was used to continuously analyze flowing aqueous ethanol–glucose solutions by automatically determining the resonance wavelengths of the hydrogel and reference area, which were plotted in a sensorgram over time. From the recorded sensorgrams, the resonance wavelength shifts for various ethanol–glucose–water solutions were determined by referencing the specific resonance wavelengths of the individual two-component aqueous solutions (ethanol: 0–100 vol %; glucose: 0–4 vol % in double-deionized water) to a baseline (double-deionized water). More details of the used sensor setup were published in a previous work [38].

III. Methods

A. Synthesis and Determination of the Swelling Degree of the Ethanol-Sensitive Hydrogel

For hydrogel synthesis, the monomer acrylamide (15 vol %) and the cross-linker N,N'-methylenebisacrylamide (0.44 mol %) were dissolved in double-deionized water, and lithium phenyl-2,4,6-trimethylbenzoyl phosphinate (0.44 mol %) was added as photoinitiator. The polymerization was initiated with UV light. For more details regarding the hydrogel synthesis, refer to [38].

For analyzing the swelling behavior of the ethanol-sensitive hydrogel, the swelling curve of a macroscopic (650 μm $\times$ 15 mm $\times$ 15 mm) gel covalently bonded to a substrate was determined. For this, the macroscopic, cubic gel sample was placed in ethanol–water solutions with varying ethanol concentrations ranging from 0 to 100 vol % with steps of 10 vol %. At each step, the sample was equilibrated for 24 h. After equilibration, the volume change was measured by optical quantification of height and surface area change in the sample. With this, the swelling degree q was obtained as a function of the ethanol volume fraction in the solution using the relationship

$$q = \frac{V}{V_0} \tag{1}$$

where V and V_0 denote the current and the initial hydrogel volumes, respectively. For more information, refer to [38].

B. Determination of Refractive Indices of Hydrogel and Fluid

For calculation of the corresponding refractive indices from the resonance wavelength shifts $\Delta\lambda_{\mathrm{res}}$, the bulk sensitivity S of the nanostructured surfaces has to be known. This is determined from the slope of the resonance wavelength shift of the reference area over the refractive indices n of the investigated solutions determined by a refractometer (DR201-95, A. KRÜSS Optronic GmbH, Hamburg, Germany); see

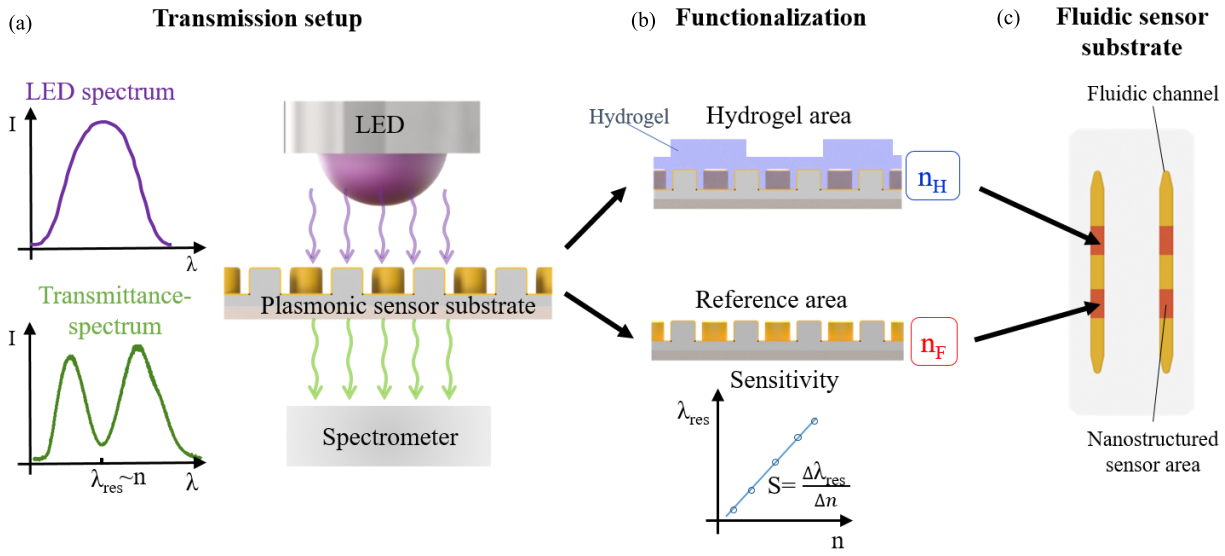

Fig. 1. Sensor setup showing (a) transmission setup and the resulting transmittance spectrum with depicted resonance wavelength λ_{res} proportional to the refractive index n. (b) Hydrogel-functionalized sensor area and a nonfunctionalized reference area for simultaneous detection of the refractive indices n_H and n_F of hydrogel and fluid, respectively. (c) Sensor substrate with fluidic channels including hydrogel and reference area.

Fig. 1, and using the relationship

$$S = \frac{\Delta\lambda_{\mathrm{res}}}{\Delta n}. \tag{2}$$

With the calculated sensitivity S and the analyzed resonance wavelength λ_{res} of hydrogel and reference area, the respective refractive index changes n_{H} and n_{F} of the hydrogel and the fluid can be determined.

C. Analytical Model for Refractive Indices of the Hydrogel–Fluid System

The simplest method to calculate the refractive index of an ideal multicomponent mixture, here the hydrogel–fluid system, is the application of the Arago–Biot equation [40], [41]. With this approach, the refractive index n_{tot} of the total mixture can be approximated by the sum of the refractive index of each constituent multiplied with their respective volume fraction

$$n_{\mathrm{tot}} = \sum_i n_i \frac{V_i}{V_{\mathrm{tot}}} = \sum_i n_i v_i \tag{3}$$

where n_i is the refractive index and V_i is the volume of component i. V_{tot} is the total volume of the mixture, and $v_i = V_i / V_{\mathrm{tot}}$ is the corresponding volume fraction. For nonideal mixtures, this model cannot be applied, since molecular interactions lead to nonlinear effects. This applies—among others—to mixtures of water and ethanol; see Fig. 2. This typical curve of the refractive index of aqueous ethanol solutions is due to the concentration-dependent interactions of molecules and thus due to anomalies of water–ethanol (WE) mixtures [42]. Here, we assume that the refractive index of a water (W)–ethanol (E)–glucose (G) mixture can be determined by application of (3) and treatment of the WE mixture as one component of the solution

$$n_{\mathrm{WEG}} = n_{\mathrm{WE}}\, v^{\mathrm{F}}_{\mathrm{WE}} + n_{\mathrm{G}}\, v^{\mathrm{F}}_{\mathrm{G}}. \tag{4}$$

Here, the superscript F denotes the fluid. It must be noted that using this approach, n_{WE} is a (known) function of ethanol concentration, rather than a constant value. The volume fraction of WE in the fluid can be evaluated using the relationship

$$v^{\mathrm{F}}_{\mathrm{WE}} = v^{\mathrm{F}}_{\mathrm{W}} + v^{\mathrm{F}}_{\mathrm{E}}. \tag{5}$$

Analogously to (4), the refractive index of a hydrogel H, consisting of a polymer matrix P, swollen in WE–glucose solution WEG, can be described by

$$\begin{aligned} n_{\mathrm{H}} &= n_{\mathrm{WEG}}\, v^{\mathrm{H}}_{\mathrm{WEG}} + n_{\mathrm{P}}\, v^{\mathrm{H}}_{\mathrm{P}} \\ &= n_{\mathrm{WE}}\, v^{\mathrm{H}}_{\mathrm{WE}} + n_{\mathrm{G}}\, v^{\mathrm{H}}_{\mathrm{G}} + n_{\mathrm{P}}\, v^{\mathrm{H}}_{\mathrm{P}} \end{aligned} \tag{6}$$

with

$$v^{\mathrm{H}}_{\mathrm{WE}} = v^{\mathrm{H}}_{\mathrm{W}} + v^{\mathrm{H}}_{\mathrm{E}}. \tag{7}$$

IV. Results and Discussion

A. Swelling Behavior of the Ethanol-Sensitive Hydrogel

To gain a better understanding of the influence of interfering constituents on the refractive index, the volume fractions of each constituent in the hydrogel and the fluid are analyzed. To evaluate (3), the swelling behavior of the ethanol-sensitive hydrogel needs to be known.

The results of the measurements of the swelling degree q as a function of ethanol are depicted in Fig. 3. The curve exhibits three distinct regions: In the first region, approximately from 0 to 30 vol % ethanol, a decrease in volume is observed with a slope of approximately $-0.014\,(\mathrm{vol}\,\%)^{-1}$. Between 30 and 50 vol % the main volume phase transition of the gel takes place with a slope of approximately $-0.024\,(\mathrm{vol}\,\%)^{-1}$. For concentrations larger than 50 vol %, only minor volume changes occur.

For the evaluation of (3), the volume fractions $v^{\mathrm{H}}_{\mathrm{P}}$ and $v^{\mathrm{H}}_{\mathrm{F}}$ of the polymer and the fluid in the hydrogel have to be known. It is assumed that the hydrogel in a pure ethanol bath is completely dehydrated, i.e., the hydrogel comprises no fluid

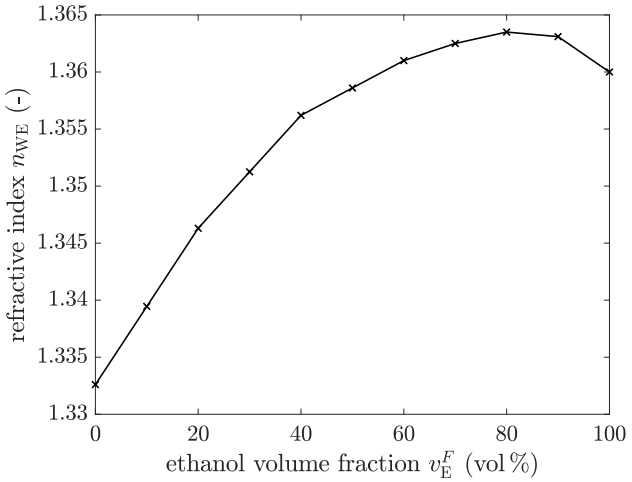

Fig. 2. Refractive index n_{WE} of WE solutions measured with a reference refractometer.

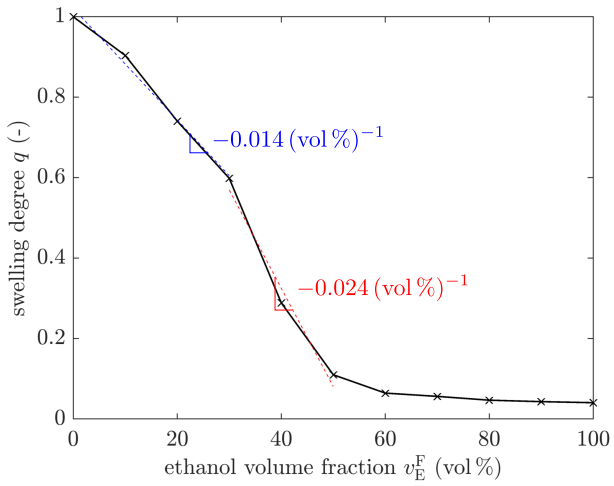

Fig. 3. Measured swelling degree $q = V/V_0$ of the hydrogel for different ethanol concentrations.

and, therefore, $v_P^H = 1$ [43]. Using this assumption, the volume fractions searched for are expressed by the relationships

$$v_P^H = \frac{q_{100}}{q} \tag{8}$$

$$v_F^H = 1 - v_P^H \tag{9}$$

with q_{100} denoting the value of the swelling degree q in pure ethanol solution ($v_E^F = 100$ vol %). For the investigation of the volume fractions in multicomponent systems (here: the aqueous WE solution), it is assumed that there are no cross-sensitivities toward nontarget substances (here: glucose) and q is only a function of the targeted substance concentration (here: ethanol). Using these assumptions, the volume fractions v_{WE}^H and v_G^H of the WE and glucose in the hydrogel can be obtained by

$$v_{WE}^H = v_{WE}^F\, v_F^H \tag{10}$$

$$v_G^H = v_G^F\, v_F^H. \tag{11}$$

In general, the sum of the volume fractions of all the constituents in the fluid and the hydrogel equals one, i.e.,

$$\sum_i v_i^H = v_P^H + v_{WE}^H + v_G^H = 1 \tag{12}$$

$$\sum_i v_i^F = v_{WE}^F + v_G^F = 1. \tag{13}$$

After the determination of the swelling degree q and using the relationships of (8), (9), and (11)–(13), all the relevant volume fractions for the WE–glucose system can be calculated; compare Fig. 4. Within the frame of this work, only solutions with up to 4 vol % glucose are considered. This investigation shows that the volume fraction of the fluid in the hydrogel v_F^H changes only slightly in the region between 0 and 30 vol % ethanol and exhibits an almost linear behavior in the region between 30 and 80 vol % ethanol. It is important to note that the main volume phase transition of the hydrogel occurs at different ethanol concentrations than the major changes in v_F^H and v_P^H; compare Figs. 3 and 4. The volume fractions of WE v_{WE}^H and glucose v_G^H within the hydrogel show a stronger influence on the glucose concentration for low ethanol concentrations. For

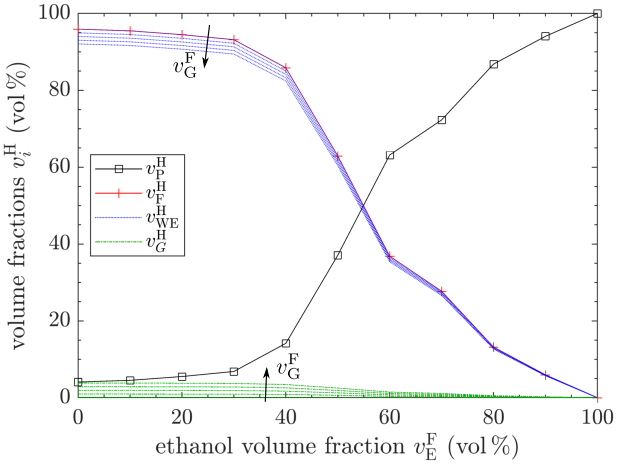

Fig. 4. Volume fractions v_i^H of the individual constituents of the hydrogel as a function of ethanol concentration v_E^F in the fluid. The arrows indicate increasing glucose volume fractions v_G^F. Investigated glucose concentrations are $v_G^F = \{0, 1, 2, 3, 4\}$ vol %.

higher ethanol concentrations, the volume fractions v_{WE}^H and v_G^H are basically independent of the glucose concentration, since the volume fraction of the fluid v_F^H in the hydrogel network is very small.

It has to be noted that the accuracy of the measured swelling curve has a strong impact on the obtained volume fractions in the hydrogel. At higher ethanol volume fractions, the swelling degree q becomes small, resulting in a high sensitivity of v_P^H and v_F^H toward measurement errors in q; compare (8).

B. Difference Method for Eliminating the Influence of Interfering Substances

The objective of this work is to create a sensor system which is able to determine the ethanol concentration in unknown mixtures comprising water, ethanol, and glucose. It is a proof-of-concept for more complex multicomponent systems and, potentially, also for the measurement of components other than ethanol. For a selective determination of individual constituents in multicomponent solutions, the influence of other

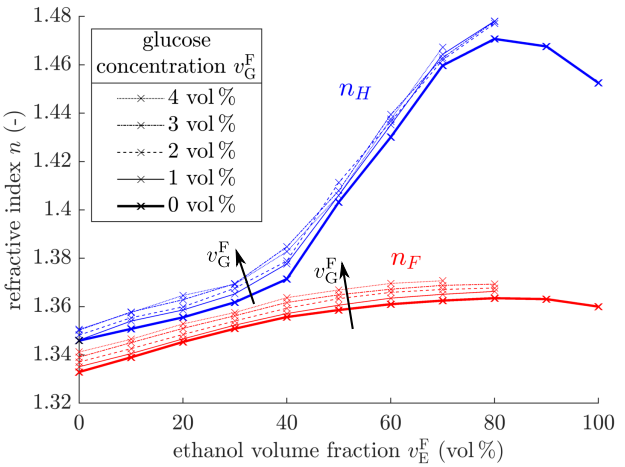

Fig. 5. Obtained refractive indices of the hydrogel n_H (blue) and the fluid n_F (red). The investigations were performed for glucose concentrations $v_G^F = \{0, 1, 2, 3, 4\}$ vol %. The increase in glucose concentration is indicated with arrows and also marked using different line styles as given in the legend.

substances in the fluid on the refractive-index-sensitive sensor signal needs to be eliminated or at least reduced significantly.

The refractive indices of the hydrogel and the fluid are calculated from the measured resonance wavelength shifts, as described in Section III-C. The results for n_F and n_H are depicted in Fig. 5.

The solubility of glucose in ethanol–water solutions is limited for higher ethanol volume fractions. Therefore, it was not possible to determine n_F and n_H for $v_G^F \neq 0$ vol % together with $v_E^F \geq 80$ vol %.

It is observed that n_H and n_F increase with increasing glucose concentrations and—as described by (4)—the different n_F curves for the investigated glucose concentrations $v_G^F = \{0, 1, 2, 3, 4\}$ vol % glucose are parallel-shifted to each other. Similar to n_{WE}, the refractive index n_F shows increases with increasing ethanol concentrations until an ethanol concentration of around 70 vol % and then decreases with increasing ethanol concentration; compare Figs. 2 and 5.

The refractive index n_H shows a different trend with respect to glucose concentration. For low ethanol concentrations ($v_E^F \leq 30$ vol %), the graphs are also parallel-shifted for increasing glucose concentrations, exhibiting a similar behavior like n_F. But for ethanol concentration above 30 vol %, the slope increases and the distance between the different curves of n_H decreases. Due to limited solubility of glucose in ethanol, above 80 vol % ethanol, we were only able to determine n_H for $v_G^F = 0$ vol %. For these high ethanol concentrations, a decrease of n_H is observed.

It must be emphasized that for low ethanol concentrations ($v_E^F \leq 30$ vol %), the change in the refractive indices n_H and n_F is almost equal and shows that the refractive index of the hydrogel behaves like the refractive index of the fluid in this range. This is due to the fact that the fluid fraction in the hydrogel v_F^H dominates in this range; see Fig. 4. Above 30 vol % ethanol, the volume fraction v_P^H of the polymer in the hydrogel increases, and therefore, the polymer has a stronger influence on the overall refractive index, resulting in a steeper slope of n_H. The decreasing volume fraction v_F^H with increasing ethanol concentration (30 vol % $< v_E^F <$ 80 vol %) also reduces the influence of glucose.

Based on the obtained values for $n_F = n_{WEG}$ and evaluation of (4), a refractive index $n_G \approx 1.55$ for glucose is obtained. To determine the concentration of ethanol, the influence of glucose on the measurement signal of n_H should be eliminated or the signal should be reduced to the ethanol-induced swelling degree q. Here, we propose to use the difference $n_{diff} = n_H - n_F$ of the refractive indices of the hydrogel and the fluid as input signal. The corresponding curve is depicted in Fig. 6. Using (4) and (6), we obtain

$$n_{diff} = n_{WE}\left(v_{WE}^H - v_{WE}^F\right) + n_G\left(v_G^H - v_G^F\right) + n_P v_P^H \quad (14)$$

showing the relationship between n_{diff} and the individual volume fractions and refractive indices of the respective constituents. It is assumed that n_{WE}, $(v_{WE}^H - v_{WE}^F)$, n_G, n_P, and v_P^H are independent of glucose concentration. Therefore, the influence of glucose on n_{diff} is small if $(v_G^H - v_G^F)$ is small. This term is almost zero in the range of 0–30 vol % and marginal between 30 and 70 vol % ethanol. For higher ethanol concentrations ($v_E^F \geq 80$ vol %), the influence of glucose is not reduced, but the influence of glucose on the refractive index of the hydrogel is small, since v_G^H becomes very small. In the range of 40–70 vol % ethanol, a linear relationship between n_{diff} and v_E^F can be assumed

$$n_{diff} \approx m\, v_E^F + n. \quad (15)$$

Therefore, n_{diff} can be used to infer ethanol concentration

$$v_E^F \approx \frac{n_{diff} - n}{m} \quad (16)$$

with $m = 0.0026\,(\text{vol}\,\%)^{-1}$ and $n = -0.0836$. For the range of 40–80 vol %, a polynomial fit

$$n_{diff} \approx a_1 + a_2 v_E^F + a_3 \left(v_E^F\right)^2 \quad (17)$$

suits the respective data. Therefore, ethanol concentration can be obtained by

$$v_E^F \approx -\frac{a_2}{2a_3} \pm \sqrt{\left(\frac{a_2^2}{4a_3^2} - \frac{a_1 - n_{diff}}{a_3}\right)} \quad (18)$$

with $a_1 = -0.1262$, $a_2 = 0.0041\,(\text{vol}\,\%)^{-1}$, and $a_3 = -1.6062 \cdot 10^{-5}(\text{vol}\,\%)^{-2}$.

As can be concluded from Fig. 6, the working range for ethanol is limited to 40–80 vol %. Below 40 vol %, n_{diff} is nearly constant, while above 80 vol %, n_{diff} is not monotonously increasing anymore. Here, multiple values of v_E^F are assigned to one value of n_{diff} leading to nonunique results for the determined ethanol concentration.

C. Validation of Difference Method for Selective Ethanol Determination

With the findings discussed in Section IV-B, the sensor system was calibrated by applying the difference method for selective determination of ethanol concentration. For this purpose, calibration curves for 40–80 vol % aqueous ethanol solutions were determined from the difference in resonance

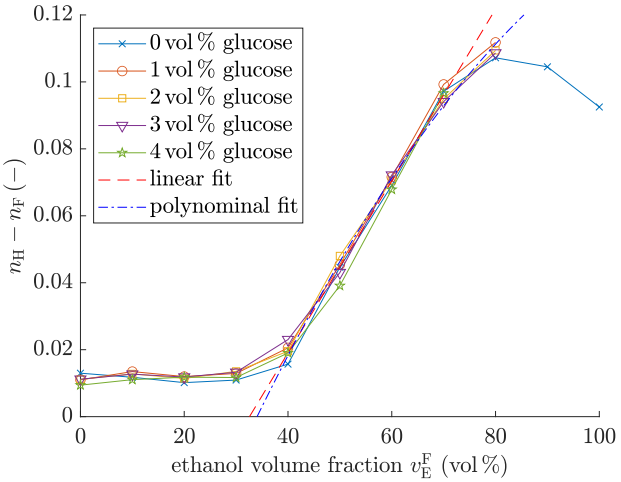

Fig. 6. Difference in obtained refractive indices of hydrogel and fluid $n_H - n_F$. The respective measurements were performed for glucose concentrations $v_G^F = \{0, 1, 2, 3, 4\}$ vol %.

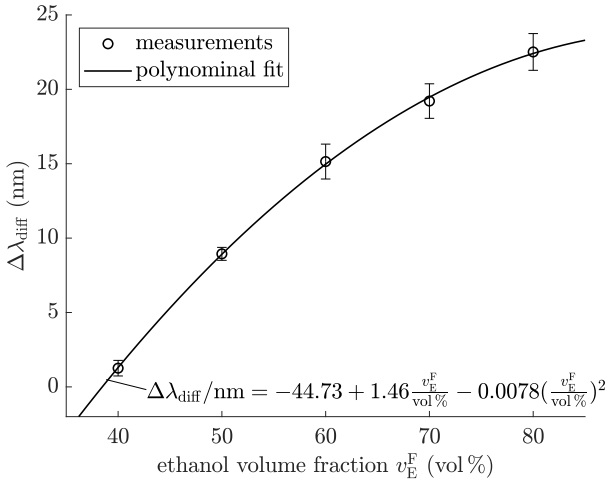

Fig. 7. Mean values and standard deviations for the resonance wavelength shift $\Delta\lambda_{diff}$ and the respective polynomial fit used as calibration curve for the selective determination of ethanol concentration.

wavelength shift of hydrogel $\Delta\lambda_{res}^H$ (hydrogel area) and fluid $\Delta\lambda_{res}^F$ (reference area)

$$\Delta\lambda_{diff} = \Delta\lambda_{res}^H - \Delta\lambda_{res}^F. \tag{19}$$

For the determination of the calibration curve, λ_{diff} was determined by averaging five successive measurements of each data point between 40 and 80 vol %. Here, it should be emphasized that the resonance wavelength shifts $\Delta\lambda_{res}^H$ and $\Delta\lambda_{res}^F$ are proportional to the formally used refractive indices n_F and n_H. The calibration of the system is conducted using a polynomial fit for the $\Delta\lambda_{diff}$ curve for an ethanol concentration range of 40–80 vol %; see Fig. 7. To demonstrate the usability of the proposed difference method, the ethanol volume fraction v_E^F is determined for different ethanol–water–glucose solutions. For performance evaluation, the determined ethanol values are compared against the real ethanol concentrations of the fluid; see Fig. 8. The respective errors and standard deviations of these investigations are listed in Table I. For the used system, the mean absolute deviation in ethanol concentration determination is smaller than 2 vol % for ethanol concentrations between 40 and 70 vol %. It must be noted that the maximum working range is restricted to ethanol concentrations between 30 and 80 vol %. Below this range, the volume fraction of the polymer v_P^H in the hydrogel changes only marginally; compare Fig. 4. This leads to an almost equal change in the refractive index of the hydrogel n_H and the fluid n_F for low ethanol concentrations. Thus, n_{diff} is almost constant and the determination of the corresponding ethanol concentration is not feasible with the used hydrogel. For ethanol concentrations above 80 vol %, the prediction accuracy for the ethanol concentration reduces significantly for multicomponent solutions. According to Fig. 4, only a very small liquid fraction remains in the gel at higher ethanol concentrations. The volume fraction v_G^H of glucose in the hydrogel becomes much smaller than v_G^F, and the glucose-dependent term $(v_G^H - v_G^F)$ is not negligible anymore. As a result, the error between the predicted and real ethanol concentrations in the liquid becomes larger. Therefore, for this proof-of-concept, the difference method should not be applied for ethanol concentrations above 70 vol % or below 30 vol %.

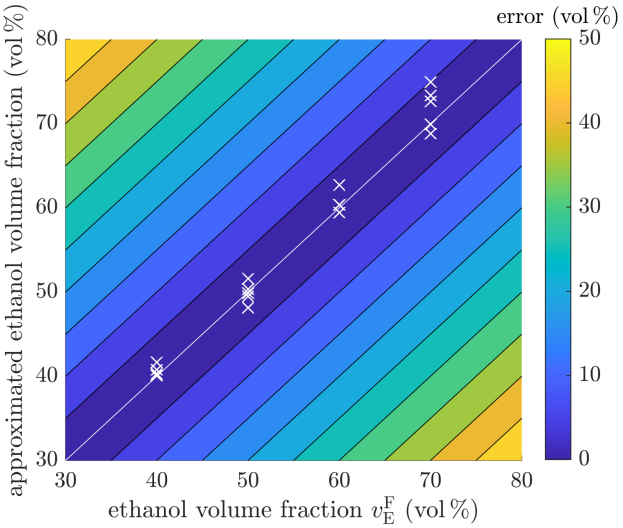

Fig. 8. Approximation of the ethanol concentration v_E^F based on a polynomial fit.

TABLE I
PREDICTION ERRORS AND STANDARD DEVIATIONS FROM THE DETERMINATION OF THE ETHANOL VOLUME FRACTION v_E^F IN AQUEOUS ETHANOL–GLUCOSE SOLUTIONS

v_E^F (vol %)	mean absolute error (vol %)	mean relative error (%)	standard deviation (vol %)
40	-0.58	-1.46	0.67
50	0.11	0.22	1.26
60	-0.47	-0.78	1.34
70	-1.95	-2.78	2.51

V. CONCLUSION AND OUTLOOK

Based on recent advancements in hydrogel-based plasmonic sensor technology, this study describes the development of a method to reliably determine the concentration of a specific target substance in complex liquid environments without being influenced by interfering substances. In the context of a

proof-of-concept, the selective determination of the ethanol concentration in aqueous ethanol–glucose solutions using a plasmonically active sensor substrate functionalized with an ethanol-sensitive hydrogel was performed. To obtain ethanol concentration of the fluid, a difference method is developed and applied, with the simultaneously measured resonance wavelength shifts of the fluid (reference area) and the hydrogel (hydrogel-functionalized area) as input.

A major objective of this research was to develop and validate this difference method as a reliable means of determining the concentration of a target substance in complex liquid environments without being influenced by interfering substances. We confirmed its applicability by quantifying the ethanol concentration amidst the presence of the interfering substance glucose within the solution.

The independence of the result regarding glucose was investigated through analytical modeling of the refractive index of the hydrogel and the liquid, based on the assumptions of the Arago and Biot model [40]. The developed model accounts for the volume fractions of water, ethanol, glucose, and polymer within the hydrogel, requiring knowledge of the hydrogel's swelling curve.

Our analytical and experimental results confirm that at low glucose concentrations, the impact of glucose on the difference in the refractive indices n_{diff} or the proportional resonance wavelength shifts (λ_{diff}) is negligible, making it a reliable indicator of ethanol concentration.

This independence of $\Delta\lambda_{\mathrm{diff}}$ upon glucose results if the volume fraction of the interfering substances (here: glucose) is equal in the fluid and the hydrogel. For the investigated system, this requirement is fulfilled for low ethanol concentrations (below 30 vol %). For ethanol concentrations above 30 vol % and below 70 vol %, the dependence on glucose is still significantly reduced. It is shown that by applying the difference method in the working range between 30 and 70 vol%, the ethanol concentration of aqueous ethanol–glucose solutions could be reliably determined.

At ethanol concentrations below 30 vol %, the refractive index of the hydrogel behaves similar to the refractive index of the fluid, since the volume fractions of fluid and polymer in the hydrogel do not change significantly. For this reason, lower ethanol concentrations cannot be determined with the here used ethanol-sensitive hydrogel. Furthermore, this also means that the limitation of the working range for low ethanol volume fractions below 30 vol % is not due to the difference method, but to the swelling behavior of the hydrogel used. This finding refuted our previous assumption in [38] that the limitation of the working range was due to the near-surface sensitivity, with significant source defects being detectable only above 40 vol %. The ethanol-sensitive hydrogel can easily be chemically modified. It might be possible to create a similar system to detect a lower ethanol concentration if the composition of monomer, cross-linker, and photo-initiator is changed.

In summary, the presented sensor system combined with the proposed difference method shows a working range of 40–70 vol % ethanol for selective determination of ethanol. Here, we tested the system with small concentrations of interfering substances. Therefore, the method should be analyzed regarding its performance for higher concentrations of interfering nontarget constituents.

Further research efforts should focus on validating the proposed difference method using a diverse range of multicomponent solutions, spanning various fluid compositions and constituent concentrations. In addition, investigating different stimuli-responsive hydrogels and their compatibility with the sensor system is essential. In addition, incorporating two or more distinct hydrogels within the system presents a realistic opportunity for enabling simultaneous detection of multiple target substances. This approach could significantly enhance the sensor's versatility and broaden its applicability across a wide range of monitoring scenarios.

To assess the sensor's performance, it is necessary to conduct thorough examinations of accuracy, reproducibility, and long-term stability, considering various factors such as the influence of environmental conditions, potential degradation of sensor components over time, and the occurrence of drift in sensor readings. These further investigations are required to ensure reliable and consistent sensor operation over extended periods and under varying operating conditions. Additional detailed analysis of the sensor response to different stimuli and its ability to maintain accuracy and reproducibility across a range of operating conditions will provide more reliable statements on sensor's effectiveness and suitability for real-world applications.

REFERENCES

[1] X. Chen et al., "Progress and prediction of multicomponent quantification in complex systems with practical LC-UV methods," *J. Pharmaceutical Anal.*, vol. 13, no. 2, pp. 142–155, Feb. 2023, doi: 10.1016/j.jpha.2022.11.011.

[2] A. R. Mansur, J. Oh, H. S. Lee, and S. Y. Oh, "Determination of ethanol in foods and beverages by magnetic stirring-assisted aqueous extraction coupled with GC-FID: A validated method for halal verification," *Food Chem.*, vol. 366, Jan. 2022, Art. no. 130526, doi: 10.1016/j.foodchem.2021.130526.

[3] K. Y. Kavittha, G. Geetha, and R. Venkatnarayanan, "Development and validation of liquid chromatographic methods for the estimation of drugs in multi-component dosage forms," *J. Pharmacie Globale*, vol. 3, no. 11, pp. 1–10, 2012.

[4] A. V. Kostarnoi, G. B. Golubitskii, E. M. Basova, E. V. Budko, and V. M. Ivanov, "High-performance liquid chromatography in the analysis of multicomponent pharmaceutical preparations," *J. Anal. Chem.*, vol. 63, no. 6, pp. 516–529, Jun. 2008, doi: 10.1134/s1061934808060026.

[5] M. Sobczyk, S. Wiesenhütter, J. R. Noennig, and T. Wallmersperger, "Smart materials in architecture for actuator and sensor applications: A review," *J. Intell. Mater. Syst. Struct.*, vol. 33, no. 3, pp. 379–399, Feb. 2022, doi: 10.1177/1045389x211027954.

[6] Y. Feng et al., "Real-time and on-line monitoring of ethanol fermentation process by viable cell sensor and electronic nose," *Bioresources Bioprocessing*, vol. 8, no. 1, pp. 1–10, Dec. 2021, doi: 10.1186/s40643-021-00391-5.

[7] O. M. Istrate, L. Rotariu, and C. Bala, "A novel amperometric biosensor based on poly(allylamine hydrochloride) for determination of ethanol in beverages," *Sensors*, vol. 21, no. 19, p. 6510, Sep. 2021, doi: 10.3390/s21196510.

[8] M. Abdolrazzaghi, N. Kazemi, V. Nayyeri, and F. Martin, "AI-assisted ultra-high-sensitivity/resolution active-coupled CSRR-based sensor with embedded selectivity," *Sensors*, vol. 23, no. 13, p. 6236, Jul. 2023, doi: 10.3390/s23136236.

[9] R. Boroujerdi, A. Abdelkader, and R. Paul, "Highly selective detection of ethanol in biological fluids and alcoholic drinks using indium ethylenediamine functionalized graphene," *Sensors Diag.*, vol. 1, no. 3, pp. 566–578, 2022, doi: 10.1039/d2sd00011c.

[10] M. Baghelani, "Wide-band label-free selective microwave resonator-based sensors for multi-component liquid analysis," *IEEE Sensors J.*, vol. 22, no. 3, pp. 2128–2134, Feb. 2022, doi: 10.1109/JSEN.2021.3137275.

[11] N. Hosseini and M. Baghelani, "Selective real-time non-contact multi-variable water-alcohol-sugar concentration analysis during fermentation process using microwave split-ring resonator based sensor," *Sens. Actuators A, Phys.*, vol. 325, Jul. 2021, Art. no. 112695, doi: 10.1016/j.sna.2021.112695.

[12] S. Kasemsumran et al., "Simultaneous monitoring of the evolution of chemical parameters in the fermentation process of pineapple fruit wine using the liquid probe for near-infrared coupled with chemometrics," *Foods*, vol. 11, no. 3, p. 377, Jan. 2022, doi: 10.3390/foods11030377.

[13] R. J. A. do Nascimento, G. R. de Macedo, E. S. dos Santos, and J. A. de Oliveira, "Real time and in situ near-infrared spectroscopy (Nirs) for quantitative monitoring of biomass, glucose, ethanol and glycerine concentrations in an alcoholic fermentation," *Brazilian J. Chem. Eng.*, vol. 34, no. 2, pp. 459–468, Apr. 2017, doi: 10.1590/0104-6632.20170342s20150347.

[14] H. Huang, H. Yu, H. Xu, and Y. Ying, "Near infrared spectroscopy for on/in-line monitoring of quality in foods and beverages: A review," *J. Food Eng.*, vol. 87, no. 3, pp. 303–313, Aug. 2008, doi: 10.1016/j.jfoodeng.2007.12.022.

[15] Y. Sasaki, X. Lyu, W. Tang, H. Wu, and T. Minami, "Supramolecular optical sensor arrays for on-site analytical devices," *J. Photochemistry Photobiol. C, Photochemistry Rev.*, vol. 51, Jun. 2022, Art. no. 100475, doi: 10.1016/j.jphotochemrev.2021.100475.

[16] R. Umapathi et al., "Colorimetric based on-site sensing strategies for the rapid detection of pesticides in agricultural foods: New horizons, perspectives, and challenges," *Coordination Chem. Rev.*, vol. 446, Nov. 2021, Art. no. 214061, doi: 10.1016/j.ccr.2021.214061.

[17] Q. Wei, Q. Dong, and H. Pu, "Multiplex surface-enhanced Raman scattering: An emerging tool for multicomponent detection of food contaminants," *Biosensors*, vol. 13, no. 2, p. 296, Feb. 2023, doi: 10.3390/bios13020296.

[18] J. Sun, L. Gong, W. Wang, Z. Gong, D. Wang, and M. Fan, "Surface-enhanced Raman spectroscopy for on-site analysis: A review of recent developments," *Luminescence*, vol. 35, no. 6, pp. 808–820, Sep. 2020, doi: 10.1002/bio.3796.

[19] Y. Zhao, Q.-L. Wu, and Y.-N. Zhang, "Simultaneous measurement of salinity, temperature and pressure in seawater using optical fiber SPR sensor," *Measurement*, vol. 148, Dec. 2019, Art. no. 106792, doi: 10.1016/j.measurement.2019.07.020.

[20] S. K. Srivastava, R. Verma, and B. D. Gupta, "Surface plasmon resonance based fiber optic sensor for the detection of low water content in ethanol," *Sens. Actuators B, Chem.*, vol. 153, no. 1, pp. 194–198, Mar. 2011, doi: 10.1016/j.snb.2010.10.038.

[21] M. Li, R. Singh, Y. Wang, C. Marques, B. Zhang, and S. Kumar, "Advances in novel nanomaterial-based optical fiber biosensors—A review," *Biosensors*, vol. 12, no. 10, p. 843, Oct. 2022, doi: 10.3390/bios12100843.

[22] W. Zhang, R. Singh, F.-Z. Liu, C. Marques, B. Zhang, and S. Kumar, "WaveFlex biosensor: A flexible-shaped plasmonic optical fiber sensor for histamine detection," *IEEE Sensors J.*, vol. 23, no. 19, pp. 22533–22542, Oct. 2023, doi: 10.1109/JSEN.2023.3305464.

[23] X. Liu, R. Singh, G. Li, C. Marques, B. Zhang, and S. Kumar, "WaveFlex biosensor-using novel tri-tapered-in-tapered four-core fiber with multimode fiber coupling for detection of aflatoxin b1," *J. Lightw. Technol.*, vol. 41, no. 24, pp. 7432–7442, Dec. 2023, doi: 10.1109/jlt.2023.3301069.

[24] N. Steinke, S. Döring, R. Wuchrer, C. Kroh, G. Gerlach, and T. Härtling, "Plasmonic sensor for on-site detection of diclofenac molecules," *Sens. Actuators B, Chem.*, vol. 288, pp. 594–600, Jun. 2019, doi: 10.1016/j.snb.2019.02.069.

[25] C. Kroh, R. Wuchrer, N. Steinke, M. Guenther, G. Gerlach, and T. Härtling, "Hydrogel-based plasmonic sensor substrate for the detection of ethanol," *Sensors*, vol. 19, no. 6, p. 1264, Mar. 2019, doi: 10.3390/s19061264.

[26] R. Wuchrer, S. Amrehn, L. Liu, T. Wagner, and T. Härtling, "A compact readout platform for spectral-optical sensors," *J. Sensors Sensor Syst.*, vol. 5, no. 1, pp. 157–163, May 2016, doi: 10.5194/jsss-5-157-2016.

[27] R. Wuchrer, "Kompakte Abfrageeinheit auf Basis einer Doppelphotodiode für die Doppelphotodiode für die spektraloptische Sensorik," Ph.D. dissertation, Fac. Elect. Comput. Eng., TU Dresden, Dresden, Germany, 2019.

[28] G. Gerlach, M. Guenther, and T. Härtling, "Hydrogel-based chemical and biochemical sensors—A review and tutorial paper," *IEEE Sensors J.*, vol. 21, no. 11, pp. 12798–12807, Jun. 2021, doi: 10.1109/JSEN.2020.3042988.

[29] S. Binder and G. Gerlach, "Performance of force-compensated chemical sensors based on bisensitive hydrogels," *Sens. Actuators B, Chem.*, vol. 342, Sep. 2021, Art. no. 129420, doi: 10.1016/j.snb.2020.129420.

[30] J. Erfkamp, M. Guenther, and G. Gerlach, "Hydrogel-based sensors for ethanol detection in alcoholic beverages," *Sensors*, vol. 19, no. 5, p. 1199, Mar. 2019, doi: 10.3390/s19051199.

[31] Y. Shi and T. Wallmersperger, "Poromechanical modeling of fluid penetration in chemo-responsive gels: Parameter optimization and applications," *J. Intell. Mater. Syst. Struct.*, vol. 35, no. 3, pp. 302–314, Feb. 2024, doi: 10.1177/1045389x231201039.

[32] A. D. Drozdov, "Mechanical behavior of temperature-sensitive gels under equilibrium and transient swelling," *Int. J. Eng. Sci.*, vol. 128, pp. 79–100, Jul. 2018, doi: 10.1016/j.ijengsci.2018.03.009.

[33] J. M. Huyghe, M. M. Molenaar, and F. P. T. Baajens, "Poromechanics of compressible charged porous media using the theory of mixtures," *J. Biomechanical Eng.*, vol. 129, no. 5, p. 776, 2007, doi: 10.1115/1.2768379.

[34] B. Loret and N. Khalili, "A three-phase model for unsaturated soils," *Int. J. Numer. Anal. Methods Geomech.*, vol. 24, no. 11, pp. 893–927, 2000, doi: 10.1002/1096-9853(200009)24:11<893::AID-NAG105>3.0.CO;2-V.

[35] M. Sobczyk and T. Wallmersperger, "Modeling and simulation of the electro-chemical behavior of chemically stimulated polyelectrolyte hydrogel layer composites," *J. Intell. Mater. Syst. Struct.*, vol. 27, no. 13, pp. 1725–1737, Aug. 2016, doi: 10.1177/1045389x15606997.

[36] P. Leichsenring and T. Wallmersperger, "Modeling and simulation of the chemically induced swelling behavior of anionic polyelectrolyte gels by applying the theory of porous media," *Smart Mater. Struct.*, vol. 26, no. 3, Mar. 2017, Art. no. 035007, doi: 10.1088/1361-665x/26/3/035007.

[37] W. Ehlers and J. Bluhm, *Porous Media: Theory, Experiments and Numerical Applications*. Berlin, Germany: Springer, 2002.

[38] J. Herzog, M. Rio, C. Schuster, T. Härtling, and G. Gerlach, "Hydrogelbasierte plasmonische sensoren zur ethanoldetektion: Einfluss des quellverhaltens auf das optische signal," *TM Technisches Messen*, vol. 90, no. 12, pp. 801–809, Dec. 2023, doi: 10.1515/teme-2023-0081.

[39] G. P. Wiederrecht, *Handbook of Nanoscale Optics and Electronics*, 1st ed. Amsterdam, The Netherlands: Elsevier, 2010.

[40] D. Arago and J. Biot. (1806). *Mémoires de l'Institut des Sciences et Arts Sciences Math. et Phys*. Paris, France. [Online]. Available: https://www.biodiversitylibrary.org/item/86732

[41] Y. Shindo and K. Kusano, "Densities and refractive indices of aqueous mixtures of alkoxy alcohols," *J. Chem. Eng. Data*, vol. 24, no. 2, pp. 106–110, Apr. 1979.

[42] Q. Dong, C. Yu, L. Li, L. Nie, D. Li, and H. Zang, "Near-infrared spectroscopic study of molecular interaction in ethanol-water mixtures," *Spectrochimica Acta A, Mol. Biomolecular Spectrosc.*, vol. 222, Nov. 2019, Art. no. 117183, doi: 10.1016/j.saa.2019.117183.

[43] S. Haefner et al., "Chemically controlled micro-pores and nano-filters for separation tasks in 2D and 3D microfluidic systems," *RSC Adv.*, vol. 7, no. 78, pp. 49279–49289, 2017, doi: 10.1039/c7ra07016k.

Julia Herzog received the Diploma degree in process engineering and natural materials technology from TU Dresden, Dresden, Germany, in 2019.

Since 2020, she has been the Ph.D. student in Prof. Gerlach's Institute for Solid-State Electronics Laboratory with the TU Dresden and part of the German Research Foundations [Deutsche Forschungsgemeinschaft (DFG)] Research Training Group 1865 for "Hydrogel-based Microsystems". Her research interest relates to hydrogel-based chemical sensors for on-site detection of liquid parameters in cooperation with Prof. Härtling and Dr. Schuster's group at Fraunhofer IKTS, Dresden.

Martin Sobczyk received the Diploma and Ph.D. degrees from TU Dresden, Dresden, Germany, in 2014 and 2018, respectively. He specialized in the field of numerical modeling and simulation of intelligent materials.

In 2018, he co-developed an operator assistance system for packaging machines based on methods of machine learning with Fraunhofer Institute for Process Engineering and Packaging IVV, Dresden, Germany. Since 2019, he has been a Research Assistant with the Institute of Solid Mechanics, TU Dresden. His research interests cover numerical modeling and simulation of intelligent and nonconventional materials and structures involving multifield couplings.

Christiane Schuster received the Diploma degree in mechatronics engineering and the Ph.D. degree from TU Dresden, Dresden, Germany, in 2010, specializing in the fabrication and characterization of bio-templated nanostructures.

Since 2011, she has performed applied research in the Fraunhofer Society in the field of optical characterization of nanostructures and their development into robust sensors for test and diagnosis methods. She is the Head of the Group "Optical Test Methods and Nanosensors" with Fraunhofer Institute for Ceramic Technologies and Systems IKTS, Dresden.

Thomas Härtling received the Diploma and Ph.D. degrees in physics from TU Dresden, Dresden, Germany, in 2004 and 2008, respectively.

Since 2010, he has been with the Fraunhofer Society leading a group dealing with "optical testing and nano sensors," Fraunhofer Institute for Ceramic Technologies and Systems IKTS, Dresden. Since 2010, he has also been with TU Dresden, where he was a Professor of Nanotechnology and Nanosensors with the Department of Electrical Engineering and Information Technology, in 2018. From 2020 to 2023, he was the Director of the Fraunhofer Portugal Center for Smart Agriculture and Water Management AWAM, Vila Real, Portugal. His research interests include sensor and measurement approaches for process-integrated production monitoring based on nanoscale optical materials and structures with a focus on environmental technology, agriculture, and production-integrated measurements.

Thomas Wallmersperger received the Ph.D. and Habilitation degrees from the University of Stuttgart, Stuttgart, Germany, in 2003 and 2010, respectively.

In 2005 and 2006, he conducted research stays as a Visiting Professor with the Center for Intelligent Material Systems and Structures, Virginia Polytechnic Institute and State University, Blacksburg, VA, USA, in the field of "electroactive ionic polymers" with Prof. Donald J. Leo and Prof. Daniel J. Inman. In 2011, he became a Full Professor of Mechanics of Multifunctional Structures with TU Dresden, Dresden, Germany. He has been the Associate Dean of the Faculty of Mechanical Science and Engineering, TU Dresden, since 2016. From 2016 to 2019, he was also the Director of the Institute of Solid Mechanics. Since 2000, he has published more than 150 conference and journal articles. His research topics comprise coupled multifield problems, adaptive materials and smart structures, modeling and simulation of soft and hard materials, discretization, and numerical modeling.

Prof. Wallmersperger is an Associate Editor of the "*Journal of Intelligent Material Systems and Structures*," an Editorial Advisory Board Member of "*Acta Mechanica*," an Advisory Committee Member of the International Symposium on "Design, Modeling and Experiments of Adaptive Structures and Smart Systems," and a Program Committee Member for the SPIE-Conference "Electroactive Polymer Actuators and Devices (EAPAD)." He has been a reviewer for multiple scientific journals and an organizer of the "Second International Symposium on Design, Modeling and Experiments of Adaptive Structures and Smart Systems (DeMEASS II)" and DeMEASS VII.

Gerald Gerlach received the M.Sc. and Dr.-Ing. degrees in electrical engineering from TU Dresden, Dresden, Germany, in 1983 and 1987, respectively.

From 1983 to 1991, he worked in research and development in the field of sensors and measuring devices for several companies. In 1993, he became a Full Professor with the Department of Electrical and Computer Engineering, TU Dresden, where he was the Head of the Solid-State Electronics Laboratory from 1996 to 2024. He was the Vice President and the President of EUREL (The Convention of National Societies of Electrical Engineers of Europe), from 2007 to 2008. From 2002 to 2009, he served as a member for the Advisory Board of the VDE (German Association of Engineers in Electrical Engineering, Electronics, Information Technology). From 2007 to 2010, he served as the President for the German Society for Measurement and Automatic Control (GMA). From 2021 to 2023, he was the Head of the DFG Research Training Group "Hydrogel-based Microsystems." He has coauthored more than 300 articles in scientific journals. He is coauthor or coeditor of 11 textbooks and monographies. He is also an inventor or a co-inventor of more than 50 patents. More than 80 Ph.D. students have earned their doctorate under his supervision. His research interests include sensor and semiconductor technology, simulation and modeling of micromechanical devices, and development of solid-state sensors, especially pyroelectric infrared sensors and piezoresistive chemical sensors, and polymer-based actuators.

Dr. Gerlach served as an Associate Editor-in-Chief for the IEEE SENSORS JOURNAL from 2012 to 2021.